Qualitative and quantitative analyses in sulfated glycosaminoglycans, chondroitin sulfate/dermatan sulfate, during 3T3-L1 adipocytes differentiation

Danang Dwi CAHYADI
Tottori University
Katsuhiko WARITA
Tottori University
Naoko TAKEDA-OKUDA
Tottori University
Jun-ichi TAMURA
Tottori University
Yoshinao Z. HOSAKA (hosaka@agr.kyushu-u.ac.jp)
Kyushu University

Research Article

Keywords: 3T3-L1, adipocytes, adipogenesis, chondroitin sulfate, glycosaminoglycans, sulfotransferase

Posted Date: August 15th, 2023

DOI: https://doi.org/10.21203/rs.3.rs-3244504/v1

Abstract

Chondroitin sulfate/dermatan sulfate (CS/DS) is a member of glycosaminoglycans (GAGs) found in animal tissues. Major CS/DS subclasses, O, A, C, D, and E units, exist based on the sulfation pattern in d-glucuronic acid (GlcA) and *N*-acetyl-d-galactosamine (GalNAc) repeating units. Dermatan sulfate (DS) chains are formed when GlcA is epimerized into l-iduronic acid (IdoA). Our study aimed to analyze the CS/DS profile in 3T3-L1 cells before and after adipogenic induction. Their CS/DS contents, molecular weight (Mw), and sulfation pattern were analyzed by using a high-performance liquid chromatography system. CS/DS synthesis/degradation- and sulfotransferase-related gene expression was also analyzed by reverse transcription real-time PCR. The CS/DS amount was significantly decreased in the differentiated (DI) group compared to the non-differentiated (ND) group, along with a lower expression of CS biosynthesis-related genes, chondroitin sulfate *N*-acetylgalactosaminyltransferase 1, chondroitin sulfate *N*-acetylgalactosaminyltransferase 2, and chondroitin polymerizing factor. The GAGs in the DI group also showed lower Mw than those of ND. Furthermore, the A unit was the major CS/DS disaccharide in both groups, with a proportionally higher CS-A ratio in the DI group. This was consistent with the expression of carbohydrate sulfotransferase 12 that encodes chondroitin 4-*O*-sulfotransferase, for CS-A formation. Unlike the ND group, both GlcA and IdoA residues in the O unit of CS/DS from the DI group were absent. These qualitative and quantitative changes in CS/DS and CS/DS-synthases/hydrolases before and after adipocyte differentiation reveal valuable insights into adipocyte development.

Introduction

Chondroitin sulfate/dermatan sulfate (CS/DS) is a type of sulfated glycosaminoglycans (GAGs) that construct the extracellular matrix in various vertebrates and invertebrates' tissues [1] in the form of CS proteoglycans (CSPGs), which are involved in various biological events [2]. Chondroitin sulfate contains repeating disaccharide structures of d-glucuronic acid (GlcA) and *N*-acetyl-d-galactosamine (GalNAc), in the form of 4)GlcAβ(1→3)-GalNAcβ(1 structure [2–4]. Structural variations associated with the position of sulfation construct the major CS subclasses, such as O [GlcA-GalNAc], A [GlcA-GalNAc(4S)], C [GlcA-GalNAc(6S)], D [GlcA(2S)-GalNAc(6S)], and E [GlcA-GalNAc(4S6S)] units [5, 6]. The epimerization of the uronic acid, d-GlcA into l-iduronic acid (IdoA), results in the formation of DS chains, which are indicated as iO, iA, iC, iD, and iE units according to the coding system proposed by Sugahara and Mikami [5]. The detailed structure of the repeating disaccharides of CS and DS is presented in Fig. 1a.

Biosynthesis of the CS repeating disaccharide region involves several enzymes known as glycosyltransferases. Chondroitin GalNAc transferase-1 (ChGn-1) and ChGn-2 which possess both GalNAc transferases I (GalNAcT-I) and GalNAcT-II activities, respectively, catalyze the chain initiation and elongation of CS backbone [7–9]. Other glycosyltransferases, chondroitin synthase-1 (ChSy-1), ChSy-2, ChSy-3, and chondroitin polymerizing factor (ChPF), that possess GlcA transferase II (GlcAT-II) and GalNAcT-II activities, respectively, are involved in the chondroitin polymerization [10–12]. Moreover, formation of the structural variation of CS/DS chains is catalyzed by sulfotransferases and epimerases:

chondroitin 4-*O*-sulfotransferase 1 (C4ST-1), C4ST-2, C4ST-3, chondroitin 6-*O*-sulfotransferase 1 (C6ST-1), GalNAc 4-sulfate 6-*O*-sulfotransferase (GalNAc4S-6ST), uronyl 2-*O*- sulfotransferase (UST), dermatan 4-*O*-sulfotransferase 1 (D4ST-1), and glucuronyl C-5 epimerases (DS-epi1 and DS-epi2) [13]. Schematic illustrations of the CS/DS biosynthesis and sulfation pathways, as well as the related enzyme-encoding genes are shown in Fig. 1b.

Study on the content and composition of GAGs, especially CS/DS, in animal tissues has been carried out for decades on various species from both vertebrates and invertebrates [1, 14–24]. In addition, investigations of their biological roles at the cellular and molecular levels have also been carried out progressively. CS/DS is essential for the maintenance of cell proliferation and differentiation [13, 25–29]. Furthermore, the fluctuation of CS levels during cell differentiation may provide essential information for a better understanding of cell and tissue development. Interestingly, such basic knowledge could provide a potential tool in controlling cells' commitment to differentiate by manipulating the CS abundance. For example, in a previous study, Mikami et al. [30] revealed that CS amount is reduced during myogenesis, and its enforced suppression of CS promotes myogenic differentiation. Thus, in other words, factors controlling CS levels may provide therapeutic potential for muscle degeneration.

In adipose tissue development, a serial process of adipogenesis, which includes preadipocyte proliferation and differentiation, occurs and is followed by the enlargement of the lipid droplet. During adipogenesis, transcription factors such as peroxisome proliferator-activated receptor gamma (PPARg), CCAAT-enhancer-binding protein alpha (C/EBPa), and fatty acid binding protein 4 (FABP4) express to regulate adipogenesis [31]. In addition to the study in C2C12 myoblast [30], studies on GAG and gene expression profiles during tissue stem cell differentiation have been conducted in MC3T3-E1 osteoblast [32], human bone marrow mesenchymal stromal cells (hBMSCs, toward hepatocytes) [33], and murine embryonic stem cells (mESCs, toward embryoid bodies and extraembryonic endodermal cells) [34, 35]. Moreover, analysis of CSPGs expression in adipose tissue and 3T3-L1 cells adipogenesis, which is our focus in this study, has also been reported in several studies [36–39]. However, information on the detailed composition of CS types and expression profiles of CS-related genes in the 3T3-L1, the most used cell line in adipogenesis studies, is still limited. Given the role of CS in tissue stem cell proliferation and differentiation, we believe that understanding the changes in CS/DS content and composition during adipogenesis is essential to elucidate the role of CS/DS in the regulation of adipogenesis. Here, we aimed to profile the amount and composition of CS/DS in adipogenesis, as well as gene expression associated with their synthesis and degradation, to understand their trends.

Materials and Methods

Cell culture and differentiation

The 3T3-L1 mouse preadipocytes cell line (JCRB9014, RRID:CVCL_0123) was obtained from the Japanese Collection of Research Bioresources Cell Bank (JCRB Cell Bank, Osaka, Japan). Cells were cultured at 37°C under 5% CO_2 condition in the Dulbecco's modified Eagle's medium (DMEM; FUJIFILM

Wako Pure Chemical Corporation, Osaka, Japan), supplemented with 10% fetal bovine serum (FBS; Biosera, Ringmer, UK) and 1% commercial mixture of antibiotic containing penicillin and streptomycin (FUJIFILM Wako Pure Chemical Corporation), hereinafter referred to as basic culture medium. Two days after reaching the confluency, the cells proceeded without or with adipogenic induction for non-differentiated (ND) and differentiated (DI) groups, respectively. For the DI group, differentiation was started (day 0) by adding the differentiation medium, which was the basic culture medium supplemented with AdipoInducer Reagent containing 10 µg/mL insulin, 2.5 µM dexamethasone, and 0.5 mM 3-isobutyl-1-methylxanthine (Takara Bio, Shiga, Japan), for two days. The medium was then replenished with maintenance medium (basic culture medium supplemented with 10 µg/mL insulin) every two consecutive days, until day 10. A standard culture medium added with phosphate-buffered saline (PBS, pH 7.4) was used to replenish the medium for the ND group at the same time course.

For studies to determine the CS/DS amount and composition as well as the molecular weight analysis, the 3T3-L1 preadipocytes were cultured in T75 flasks and divided into two groups, ND and DI groups. Cells were harvested for analysis on day 10. For gene expression analysis using reverse transcription quantitative real-time polymerase chain reaction (RT-qPCR), cells were seeded in 12-well plates and divided into five groups at three different time courses as follows: (i) Control, confluent preadipocytes on day 0, (ii) ND and (iii) DI groups on day 5, and (iv) ND and (v) DI groups on day 10.

Oil Red O staining

Oil Red O (ORO) staining was performed on the Control group, as well as the ND and DI groups on days 5 and 10, to determine the progression of adipocyte differentiation, which was shown by lipid droplet accumulation. Cells were washed with PBS and fixed with 10% neutral-buffered formalin (pH 7.4; FUJIFILM Wako Pure Chemical Corporation) overnight at room temperature. Further, cells were stained with a freshly prepared ORO staining solution (Lipid Assay Kit; Cosmo Bio, Tokyo, Japan) according to the manufacturer's instructions. Briefly, after staining for at least 15 minutes at room temperature, ORO staining solution was removed, and the stained cells were washed with distilled water (dH_2O) three times. Images of the cells were captured using an inverted light microscope (Olympus IX71; Olympus, Tokyo, Japan). Isopropanol was used to extract the dye from the stained lipid droplets. Semi-quantitative approach by measuring the absorbance of the dye extraction using a microplate reader (Tecan Sunrise Remote, Grödig, Austria) at 492 nm was performed to quantify the amount of oil droplets.

Isolation of GAGs from the 3T3-L1

On day 10, the culture medium was aspirated from the flasks, and the cells were washed with PBS to completely remove the remaining culture medium. The PBS was then aspirated, and 3 mL of absolute ethanol (EtOH) was added to each flask. The cells were harvested by using a cell scrapper. The EtOH and the precipitates were moved to the sample tubes and dried in a desiccator equipped with a vacuum pump for 2 h. These dried samples were weighed and then proteolyzed, concisely, distilled water (8 mL/g dried sample) was added into the tube containing the dried sample and this suspension was incubated at 55°C, followed by the addition of borate buffer (0.5 M, pH 7.0, 10 mL/g dried sample) and 5% protease

(PROTIN NY100, Amano Enzyme, Nagoya, Japan) (50 mg/g dried sample). After completing the incubation for 5 days, each suspension was cooled on ice and quenched by adding the trichloroacetic acid (5%, w/v), followed by centrifugation. Sodium acetate (5%, w/v) and 4 times the volume of EtOH were added. The samples were then spined down and the EtOH was removed. To each sample, 0.5 mL of purified water was added, and the suspension was freeze-dried overnight.

Compositional analysis of CS/DS

Prior to the compositional analysis of CS/DS, 300 µL of dH_2O was added to the dried samples. The enzymatic digestion was performed by adding 100 µL of the sample substrate in a mixture of bovine serum albumin (BSA) solution (0.01 mg/µL), 250 mM Tris-HCl buffer (10 µL, pH 8.0), and chondroitinase ABC (1 mU/µL) (EC 4.2.2.4, Sigma Aldrich, Tokyo, Japan) or chondroitinase AC (1 mU/µL) (EC 4.2.2.5, IBEX Pharmaceuticals, Montreal, Canada) for 8 h at 37°C or 30°C, respectively. Unsaturated disaccharides obtained from the enzymatic digestion were filtered with centrifugal filter units (Millipore Ultrafree-MC-HV, Durapore-PVDF 0.45 µm, Merck Millipore, Carrigtwohill, Ireland). CS/DS amount and type were analyzed using high-performance liquid chromatography (HPLC) system as previously described by Yoshida et al. [40]. In the present study, the analysis was performed using HPLC Waters 616 Pump with Waters 600s Controller and Waters 2487 Dual λ Absorbance Detector (Waters Corporation, Milford, MA, USA). A volume of 25 µL of sample was injected onto a YMC-Pack PA-G column (4.6 × 250 mm, 5 µm; YMC, Kyoto, Japan) and the analysis was performed under the following conditions: isocratic conditions with eluent 16 mM NaH_2PO_4 buffer for the first 10 min followed by a linear gradient from NaH_2PO_4 buffer to 800 mM NaH_2PO_4 buffer at 25°C, flow rate of 1 mL/min, UV absorbance at 232 nm. To distinguish the HA from the CS/DS hybrid chains, the 4,5-unsaturated hexuronic acid (ΔHexA)-GalNAc and ΔHexA-GlcNAc were detected by using an HPLC system (ÄKTA Purifier, General Electric Healthcare, Boston, MA, USA), according to the method described in the previous study [41]. Briefly, analysis on 50 µL of sample was carried out on the Hypersil APS-2 columns (100 × 4.6 mm + 250 × 4.6 mm, 5 µm; Thermo Scientific, Waltham, MA, USA) in combination with the Shodex OHpak SB-G 6B guard column (6.0 ×50 mm, Showa Denko, Kanagawa, Japan), under the following conditions: isocratic at 35°C, using 9 mM of NaH_2PO_4 (pH 2.55), flow rate of 0.8 mL/min, UV absorbance at 231 nm. Calculation of the amounts of CS/DS hybrid chains and their sulfation patterns was performed by using a calibration curve based on the HPLC peak area of the standard unsaturated disaccharide (Seikagaku Corporation, Tokyo, Japan). In short, as previously described by Akatsu et al. [42], the total amount of disaccharide from chondroitinase AC digests subtracted from chondroitinase ABC digests to estimate the IdoA-containing disaccharides.

Determination of molecular weight of the GAGs

The molecular weight of the crude glycans was estimated by using size exclusion chromatography (SEC). A concentration of 1 mg/mL glycan solution in dH_2O was prepared and analyzed in a system consisting of a Shodex OHpak SB-G 6B guard column (6.0 ×50 mm, Showa Denko) followed by the Shodex OHpak SB-805 HQ analytical column (8.0 ×300 mm, Showa Denko) using 0.1 M $NaNO_3$ buffer at a flow rate 1 mL/min. This HPLC analysis was performed over an 18-min period and monitored with a refractive index

(RI) indicator. For this measurement, the result obtained from pullulan standards (Shodex Standard Pullulan Kit P-82, Showa Denko) was used to generate the molecular weight calibration curve.

RT-qPCR

The total RNA was extracted from the cells by using ISOSPIN Cell & Tissue RNA (Nippon Gene, Tokyo, Japan) and quantified by using NanoDrop 2000c Spectrophotometer (Thermo Fisher Scientific, Wilmington, DE, USA). An aliquot of each total RNA (500 ng) sample was reverse transcribed for cDNA synthesis using ReverTra Ace qPCR RT Master Mix with gDNA Remover (Toyobo, Osaka, Japan). The RT-qPCR experiments were carried out on a LightCycler® Nano Real-Time PCR Instrument using FastStart Essential DNA Green Master (Roche Diagnostics GmbH, Mannheim, Germany). Adipogenesis transcription factors, peroxisome proliferator-activated receptor gamma (*Pparg*) and fatty acid binding protein 4 (*Fabp4*), were examined to verify the adipogenic induction, in addition to the ORO staining quantitative approach. Furthermore, the following gene expression levels were analyzed: chondroitin sulfate *N*-acetylgalactosaminyltransferase 1 (*Csgalnact1*), chondroitin sulfate *N*-acetylgalactosaminyltransferase 2 (*Csgalnact2*), chondroitin sulfate synthase 1 (*Chsy1*), chondroitin polymerizing factor (*Chpf*), hyaluronoglucosaminidase 1 (*Hyal1*), hyaluronoglucosaminidase 2 (*Hyal2*), carbohydrate sulfotransferase 12 (*Chst12*), carbohydrate sulfotransferase 15 (*Chst15*), uronyl-2-sulfotransferase (*Ust*), carbohydrate sulfotransferase 14 (*Chst14*), dermatan sulfate epimerase (*Dse*), and dermatan sulfate epimerase-like (*Dsel*). Each gene expression level was normalized to that of a previously validated suitable reference gene, peptidylprolyl isomerase A (*Ppia*) [43]. Detailed information about the primer sets used in RT-qPCR reactions is presented in Table 1.

Table 1
Mouse cDNA primer sequences of the various genes used for RT-qPCR

Gene symbol	Primer sequences (5'-3')	Accession number	Product size (bp)	References of primer sequences
Pparg	5'-CAAGAATACCAAAGTGCGATCAA-3'	NM_001127330.3	69	[44]
	5'-GAGCAGGGTCTTTTCAGAATAATAAG-3'			
Fabp4	5'-TGGAAGCTTGTCTCCAGTGA-3'	NM_024406.4	121	[44]
	5'-AATCCCCATTTACGCTGATG-3'			
Csgalnact1	5'-TCTCTGGTTCCTGCTCACTGAAATA-3'	NM_001252623.1	144	[45]
	5'-TCTGCTTGGTCTGAGACTTTGGTAG-3'			
Csgalnact2	5'-TCTGCCTGGTACCTGTGTTCTGA-3'	NM_001362149.1	115	[45]
	5'-TATCTGCCTGAACATTTCGACCAA-3'			
Chsy1	5'-AACTTTCTCTTCGTGGGAGTCA-3'	NM_001081163.2	89	[46]
	5'-GGAATTGTCTTGGACCATGT-3'			
Chpf	5'-TTCGTCCCTCTCCGCTAGCTGACG-3'	NM_001001566.3	83	[45]
	5'-AAGGCGGCCGCTGTCCGACGTGTC-3'			
Hyal1	5'-TACACAGCATGCTCAGAAAG-3'	NM_008317.6	193	[47]
	5'-AGTGTCTCCATTCCAAACAG-3'			
Hyal2	5'-CGAGGACTCACGGGACTGA-3'	NM_010489.3	57	[48]
	5'-GGCACTCTCACCGATGGTAGA-3'			
Chst12	5'-ATCAGCATCACCAGCAACA-3'	NM_021528.3	138	[49]
	5'-TTGGTCATGCTGCCCTG-3'			
Chst14	5'-CCAAAGTGGCCTGCTCTAACTG-3'	NM_028117.3	100	[50]
	5'-AAGTCACTGCGGTGGTCCAT-3'			
Chst15	5'-TATGACAACAGCACAGACGG-3'	NM_029935.6	153	[51]

Gene symbol	Primer sequences (5'-3')	Accession number	Product size (bp)	References of primer sequences
	5'-TGCAGATTTATTGGAACTTGCGAA-3'			
Ust	5'-TCGTACCGTGGTCTTGCTTC-3'	NM_177387.3	148	[52]
	5'-TAAATAGGGCTGTTCGGCGG-3'			
Dse	5'-AGCACATTGCAGCTCGGCTTAC-3'	NM_172508.3	211	[53]
	5'-GCTGCCATCCTCTCCATGTAGTC-3'			
Dsel	5'-ACGTGGTCAAATGGCTTCAT-3'	NM_001081316.2	274	[53]
	5'-GCTGTGAAATCCAGGTGACAT-3'			
Ppia	5'-CAGGTCCATCTACGGAGAGA-3'	NM_008907.2	146	[54]
	5'-CATCCAGCCATTCAGTCTTG-3'			

Data analysis

All data are presented as mean ± standard deviation (SD). A significant difference between the two groups was determined using an unpaired two-tailed *t*-test, while the comparisons among the means in multiple groups were performed using a one-way analysis of variance (ANOVA) followed by a Bonferroni *post hoc* test. A P-value less than 0.05 was considered statistically significant. Statistical analyses were performed using the Microsoft Excel add-in statistical software (BellCurve for Excel version 4.02; Social Survey Research Information, Tokyo, Japan).

Results

Confirmation of the status of adipocyte differentiation

The ORO staining confirmed that 3T3-L1 cells in the DI group transformed into adipocyte-like structures and accumulated lipid droplets on days 5 and 10 after being induced to differentiate. However, cells in the ND group, like those in the control group, maintained their fibroblast-like phenotype and did not accumulate lipid droplets (Fig. 2a). This result was confirmed by semi-quantitative analysis of the absorbance for lipid droplet accumulation (Fig. 2b). In addition, as many studies revealed the cellular events that occurred during adipogenesis, we have also confirmed the surge of the mRNA expression of the adipogenesis transcription factors, *Pparg* and *Fabp4*, in the DI group on days 5 and 10 (Fig. 2c and d).

Quantitative analysis of CS/DS amount and composition

Representative chromatograms of GAG peptides after digestion with chondroitinases are shown in Fig. 3a. The amount of unsaturated CS/DS and HA disaccharides, as well as their compositions

calculated from the HPLC analysis, are summarized in Fig. 3b and c, and in Suppl. Table 1. The amount of the unsaturated disaccharides of CS/DS from the 3T3-L1 cell cultures was significantly decreased in the DI group compared to the ND group ($P < 0.01$). A measured amount of CS + DS in the cells from ND and DI groups was 0.48 ± 0.13 mg and 0.10 ± 0.03 mg, respectively. In addition to the CS/DS detected in our analysis, the HA amount in the cells from the DI group was about 90% less (0.04 ± 0.00 mg) than that of the ND group (0.46 ± 0.15 mg) ($P < 0.01$) (Fig. 3b). The composition of the unsaturated disaccharides of CS/DS in 3T3-L1 preadipocytes was revealed in our study, demonstrating the ΔA unit [GlcA-GalNAc(4S) and IdoA-GalNAc(4S)] (calculated from A + iA units) as the major CS/DS disaccharides in 3T3-L1 cell line that reached 89% and 86% in ND and DI groups, respectively (Fig. 3c). By using the adipogenic-induction medium to promote cell differentiation, our results also showed a significant change in its composition between both groups. The composition of the GlcA residues, A unit [GlcA-GalNAc(4S)], was increased in the DI group (44%), compared to the ND group (27%). Contrarily, the less IdoA residues [IdoA-GalNAc(4S)] were detected in the DI group (42%), compared to the ND one (62%). The GlcA and IdoA residues of ΔO unit, O [GlcA-GalNAc(0S)] and iO [IdoA-GalNAc(0S)] CS/DS disaccharides in non-differentiated 3T3-L1 cells were 8% and 2%, respectively. However, both O and iO units were not detectable in the DI group, suggesting the absence or possibly a very low amount of the ΔO unit presence in the differentiated 3T3-L1 cells. Moreover, only IdoA residues of ΔE unit, iE, were detected in both ND (2%) and DI groups (14%).

Molecular weight of the GAGs contained in 3T3-L1 cells

In addition to the GAG compositional analysis, the present study investigated its molecular weight. The molecular weight revealed in this study corresponds with the chain length of the GAGs. However, the estimation of this molecular weight should be considered as from the mixture of the CS/DS and HA. Lower molecular weight (Mw; 3.1 ± 0.3 kDa) was detected in the samples from the differentiating 3T3-L1 cells (DI group) with a low degree of dispersion (Mw/Mn; 2.2 ± 0.1). Contrarily, the GAGs contained in the cells from the ND group possessed the Mw value 10.3 ± 1.0 kDa with a higher degree of dispersion (Mw/Mn; 5.2 ± 0.1). Representative HPLC chromatograms and the comparative Mw between ND and DI groups are shown in Fig. 3d and e.

Expression of CS/DS-related genes in 3T3-L1 cells

To investigate the functional analysis of the CS synthesis in 3T3-L1 cells, the mRNA expressions of genes encoding glycosyltransferases that are involved in the CS biosynthesis, *Csgalnact1*, *Csgalnact2*, *Chsy1*, and *Chpf*, were examined. In the DI group, regardless of the time course, our results showed the remarkably low expression of *Csgalnact1* and *Chpf*, and considerably lower expression of both *Csgalnact2* on day 10, but not *Chsy1*, which was not altered during the differentiation compared to that of non-differentiated cells, as well as the control group (Fig. 4a–d).

Since the HPLC analysis showed a decreasing amount of CS/DS in differentiated cells, we also investigated the expression of CS hydrolases-related genes, *Hyal1* and *Hyal2.* Our results showed that *Hyal1* expression in the ND group was significantly decreased on day 10. Although *Hyal1* expression on

day 10 in the DI group was not different compared to those of the ND and DI groups on day 5 and the control group, the expression was considerably higher compared to that of the ND group on day 10 (P = 0.074). On the other hand, the expression level of *Hyal2* was not altered over the time course and by the adipogenic induction, except for its decreased expression in the DI group on day 10 compared to that of on day 5 (Fig. 4e and f).

The DI group showed a difference in the composition of the GlcA and IdoA residues of CS/DS compared to the ND group. This led us to investigate the expression of DS-epimerases-encoding genes, *Dse* and *Dsel*, which promote the formation of IdoA in the CS/DS chain [42, 55, 56]. Our study revealed that the *Dse* expression in the DI group on day 5 was decreased compared to that in the ND group, but there was no difference between both groups on day 10 (Fig. 5a). On the other hand, the DI group on day 10 exhibited a significantly lower *Dsel* expression compared to the ND group (Fig. 5b).

We have demonstrated the mRNA expression level of CS/DS sulfotransferase-related genes as shown in Fig. 5c–f. The mRNA expression level of *Chst12* was increased significantly in the DI group on day 10, supporting the result that the composition of the A unit of CS was increased. In contrast, the significantly lower expression level of *Chst14*, encoding D4ST-1, that catalyzes the sulfation to form DS-A was observed in the same group on day 5 and day 10. Our study revealed that the *Chst15* expression level on day 10 was substantially higher compared to those on day 5 and the control group. The mRNA expression level of this gene on day 10 was significantly decreased in the DI group compared to the ND group. *Ust* was generally expressed higher on day 10 compared to those on day 5 and the control group with no significant difference observed between ND and DI groups.

Discussion

Decrease in the CS/DS amount and its average molecular weight in differentiated cells

Adipogenic induction stimulated the 3T3-L1 preadipocytes to differentiate into adipocytes-like phenotypes showing accumulation of lipid droplets that was also confirmed by the surge of the *Pparg* and *Fabp4* expression in a day-dependent manner. The differentiated cells, in comparison to the undifferentiated cells, showed a lower amount of CS/DS and HA disaccharides, as well as their lower molecular weight. CSPGs have been reported to increase during the differentiation of 3T3-L1 cells [36], but it was confirmed that the large CSPG molecule level decreased after a few days, as observed at 72 h after the initiation of cell differentiation [39]. Decreasing the CSPG contents was also previously reported in the differentiated U-937-4 macrophage-like cells [57]. Moreover, a decrease in CS synthesis was also revealed in the differentiated HL-60 cell line toward granulocytes and monocytes [58, 59]. Although in this study we measured the CS/DS disaccharide under a different experimental design compared to those previous studies, it seems that the decrease in GAGs biosynthesis is a common phenomenon that occurs upon cell differentiation in some cell types including 3T3-L1 adipocytes. In addition, the average molecular weights of the GAGs detected in our study were remarkably low, they still fall within the range

of the CS/DS subclass, which was from 2 to 50 kDa [60]. Our results indicate the decrease of CS/DS biosynthesis and/or the increase of their degradation during the 3T3-L1 cell differentiation.

Decreased expression of Csgalnact1, Csgalnact2, andChpfin differentiated cells

In accordance with the decreasing of CS/DS contents, relatively lower expression of *Csgalnact1*, *Csgalnact2*, and *Chpf* was observed in the DI group compared to that of the ND group, although *Chsy1* expression remain unaltered. A similar result, decreased expression of *CSGALNACT1* gene (compared to controls), has been reported in human adipose-derived stromal cells (ASCs) at 7 and 21 days after adipogenic induction [61]. It is known that some glycosyltransferases, namely ChGn-1, ChGn-2, ChSy-1, ChSy-2, ChSy-3, and ChPF, regulate CS synthesis. These glycosyltransferases are involved in the series of events, including chain initiation and catalyze chondroitin polymerization, forming the repeating GlcA and GalNAc disaccharide residue [7, 8, 10, 62, 63]. Moreover, this complex polymerization activity in CS biosynthesis involves various combinations of the above enzymes [10, 62]. These phenomena of the decreased expression of the genes encoding glycosyltransferases strongly support the results of CS/DS analysis, in which the content was significantly decreased in the DI group. These findings suggest that during 3T3-L1 differentiation, there is a decrease in glycosyltransferase activity required in the CS biosynthesis.

CS degradation-associated Hyal1 expression

In addition to the glycosyltransferases-encoded genes expression, our study demonstrates higher expression levels of *Hyal1*, but not *Hyal2*, in the DI group than that of the ND group on day 10. Both *Hyal1* and *Hyal2* encode hyaluronidases, which have degradation activity against CS, as well as HA [64–66]. In conjunction with the results of CS/DS contents, these results may indicate the involvement of hyaluronidases, mainly HYAL1, in the occurrence of CS degradation in the differentiating cells. However, since the increase of the *Hyal1* in the DI group on day 10 was not as strong as the glycosyltransferase reduction, we suggest that the decrease of the molecular weight, as well as the amount of CS/DS, is predominantly caused by the decrease of their biosynthesis.

Decrease in Dsel expression in the differentiated cells

Both *Dse* and *Dsel* that encode DS-epi1 and DS-epi2, respectively, are detectable in 3T3-L1 cells, but their expressions tend to decrease during differentiation. As mentioned above, DS-epi1, and DS-epi2 facilitate epimerization of the GlcA residue into IdoA residue results in the formation of a DS chain [56]. Double knockout of both DS-epi1 and DS-epi2 mice showed no epimerase activity due to the complete absence of IdoA residue [53]. However, a study in the DS-epi1-null mice showed that epimerase activity is mainly regulated by DS-epi1 in several organs but the brain, which is suggested to be regulated by DS-epi2 [55]. *Dsel* expression in the mouse brain is higher than that of *Dse* and is suggested to be mainly responsible for the IdoA residue [42]. In the present study, *Dsel* expression was significantly higher in the ND group on day 10 compared to that of day 5 and control, and compared to *Dse* expression of the same group. Moreover, *Dsel* expression was significantly suppressed in the DI group, compared to the ND group on day

10, whereas *Dse* expression showed no significant difference at the same time point. Suppression of *Dsel* is linked to the decreasing of DS-epi2 activity, which may contribute to the decrease in the proportion of IdoA residue compared to GlcA residue. Here we also suggest that epimerase activity in adipose tissue is mainly regulated by DS-epi2.

Composition of CS/DS types and sulfotransferases gene expression

Compositional analysis of CS/DS types shows that the major disaccharide in the 3T3-L1 cells is ΔA unit [GlcA-GalNAc(4S) and IdoA-GalNAc(4S)]. In fact, compositions of the unsaturated disaccharides in CS vary among the cell lines, but the ΔO unit (ΔDi-0S), ΔA unit (ΔDi-4S), or ΔC unit (ΔDi-6S) are the major three disaccharides [67]. Moreover, in the present study, the ratio of GlcA residue of A unit (CS-A) was increased in the differentiated cells compared to that of the non-differentiated cells. Consistent with the increase in the GlcA residues, the present study shows an increase in *Chst12* in the differentiated cells on day 10. C4ST-2, encoded by the *Chst12* gene, is known to catalyze the sulfate transfer of chondroitin and desulfated dermatan sulfate to position 4 of the GalNAc [68], and is involved in CS-A formation. The increased *Chst12* expression in the DI group on day 10 may contribute to the increased ratio of CS-A in the DI group.

In the ND group, in addition to the major ΔA unit found, small ratio of non-sulfated CS/DS were detected, namely the O unit (GlcA-GalNAc), and iO unit (IdoA-GalNAc). However, non-sulfated CS/DS was not found in the DI group. On the other hand, the ratio of GlcA residues in the A unit (CS-A) was increased in differentiated cells. These changes suggest that sulfation at GlcA-GalNAc residues occurred and the CS/DS types were formed; it is reasonable to assume that the increase in *Chst12* promoted the formation of non-sulfated CS/DS to A unit CS/DS. Another sulfotransferase-encoding gene, *Chst14*, that encodes D4ST-1, was significantly decreased in the DI group on days 5 and 10. The decreasing expression level of *Chst14* was consistent with the genome-wide analysis in human ASCs, in which the *CHST14* gene was down-regulated on days 7, 14, and 21 post-adipogenic induction [61]. Previous studies showed that a lack of D4ST-1 activity due to the *CHST14* gene mutation causes a substantial reduction in the number of IdoA residue [69, 70]. The significant decrease in *Chst14* expression in the DI group in this experiment probably promoted the substantial reduction of IdoA residue, especially DS-A.

Furthermore, IdoA residue, but not GlcA, of the highly sulfated iE unit (DS-E) was presented in 3T3-L1 cells, with the proportion was about 5-fold higher in the differentiated cells than in non-differentiated cells. The formation of both E units of CS/DS is facilitated by GalNAc4S-6ST which catalyzes the transfer of sulfates to positions 4 and 6 of their GalNAc residue [71, 72]. On the other hand, our study shows the lower expression of *Chst15*, that encodes GalNAc4S-6ST, in the DI group compared to the ND group on day 10. These results are also consistent with the *CHST15* gene expression in human ASCs, which was reported to be downregulated on day 14 of post-adipogenic induction compared to the control group [61]. As previously mentioned, only iE, the IdoA residue of ΔE unit, was detected in the DI group. However, in the contrary, *Chst15* expression was decreased in the DI group compared to the ND group, regardless of

its relatively high expression on day 10. Thus, we suggest that the decrease of this *Chst15* expression might occurred in correlation to the decreased CS/DS amount revealed by HPLC analysis, but was not at the level of reducing GalNAc4S-6ST activity. In addition, although mRNA expression of *Ust*, which transfers a sulfate group to position 2 of GlcA and IdoA residues in CS/DS [73], was observed, there was no significant difference between the ND and DI groups. However, its product, the ΔD unit, was not detectable by HPLC analysis, suggesting that the content of the ΔD unit was very low in 3T3-L1 cells and may have been below the minimum threshold detected by HPLC analysis.

Conclusion

In this study, we showed that the A unit (ΔDi-4S) is the predominant disaccharide in CS/DS from the 3T3-L1 cell line, both in differentiated and non-differentiated cells. The present findings also confirm that the amount of CS/DS was reduced in cells undergoing differentiation. However, it was still unclear whether the CS/DS levels change along with adipocyte differentiation or whether this CS/DS biosynthesis controls adipocyte differentiation. The details of these cause-and-effect relations remain an issue to be elucidated in future studies. Nonetheless, these qualitative and quantitative changes in CS/DS before and after adipocyte differentiation revealed in our study may provide important molecular information for a detailed understanding of adipocyte differentiation.

Declarations

Acknowledgments

This research was supported by Japan Society for the Promotion of Science (JSPS) KAKENHI Grant Number JP20K06411 to YZH in a Grant-in-Aid for Scientific Research (C) and Grant Number JP19H03514 to KW in a Grant-in-Aid for Scientific Research (B).

Authors' Contributions

YZH and DDC conceived and designed the experiments. DDC performed the experiments, analyzed data, prepared figures, and wrote the first draft of the manuscript. KW, NT-O, JT, and YZH provided the technical expertise and edited the manuscript. All authors have approved the final version of the manuscript.

Data Availability

The data generated or analyzed during this study are included in this published article and its supplementary information files.

Compliance with Ethical Standards

Competing interests

The authors have no competing interests to declare that are relevant to the content of this article.

Ethical approval

This article does not contain any studies with human participants and animals.

References

1. Yamada, S., Sugahara, K., Özbek, S.: Evolution of glycosaminoglycans: Comparative biochemical study. Commun. Integr. Biol. **4**(2), 150–158 (2011). https://doi.org/10.4161/cib.4.2.14547
2. Mizumoto, S., Yamada, S., Sugahara, K.: Molecular interactions between chondroitin-dermatan sulfate and growth factors/receptors/matrix proteins. Curr. Opin. Struct. Biol. **34**, 35–42 (2015). https://doi.org/10.1016/j.sbi.2015.06.004
3. Miyachi, K., Wakao, M., Suda, Y.: Syntheses of chondroitin sulfate tetrasaccharide structures containing 4,6-disulfate patterns and analysis of their interaction with glycosaminoglycan-binding protein. Bioorg. Med. Chem. Lett. **25**(7), 1552–1555 (2015). https://doi.org/10.1016/j.bmcl.2015.02.011
4. Zhang, X., Liu, H., Yao, W., Meng, X., Li, Z.: Semisynthesis of chondroitin sulfate oligosaccharides based on the enzymatic degradation of chondroitin. J. Org. Chem. **84**(11), 7418–7425 (2019). https://doi.org/10.1021/acs.joc.9b00112
5. Sugahara, K., Mikami, T.: Chondroitin/dermatan sulfate in the central nervous system. Curr. Opin. Struct. Biol. **17**(5), 536–545 (2007). https://doi.org/10.1016/j.sbi.2007.08.015
6. Sugiura, N., Shioiri, T., Chiba, M., Sato, T., Narimatsu, H., Kimata, K., Watanabe, H.: Construction of a chondroitin sulfate library with defined structures and analysis of molecular interactions. J. Biol. Chem. **287**(52), 43390–43400 (2012). https://doi.org/10.1074/jbc.M112.412676
7. Gulberti, S., Jacquinet, J.C., Chabel, M., Ramalanjaona, N., Magdalou, J., Netter, P., Coughtrie, M.W.H., Ouzzine, M., Fournel-Gigleux, S.: Chondroitin sulfate *N*-acetylgalactosaminyltransferase-1 (CSGalNAcT-1) involved in chondroitin sulfate initiation: Impact of sulfation on activity and specificity. Glycobiology. **22**(4), 561–571 (2012). https://doi.org/10.1093/glycob/cwr172
8. Sato, T., Gotoh, M., Kiyohara, K., Akashima, T., Iwasaki, H., Kameyama, A., Mochizuki, H., Yada, T., Inaba, N., Togayachi, A., Kudo, T., Asada, M., Watanabe, H., Imamura, T., Kimata, K., Narimatsu, H.: Differential roles of two *N*-acetylgalactosaminyltransferases, CSGalNAcT-1, and a novel enzyme, CSGalNAcT-2. Initiation and elongation in synthesis of chondroitin sulfate. J. Biol. Chem. **278**(5), 3063–3071 (2003). https://doi.org/10.1074/jbc.M208886200
9. Uyama, T., Kitagawa, H., Tanaka, J., Tamura, J.I., Ogawa, T., Sugahara, K.: Molecular cloning and expression of a second chondroitin *N*-acetylgalactosaminyltransferase involved in the initiation and elongation of chondroitin/dermatan sulfate. J. Biol. Chem. **278**(5), 3072–3078 (2003). https://doi.org/10.1074/jbc.M209446200
10. Izumikawa, T., Uyama, T., Okuura, Y., Sugahara, K., Kitagawa, H.: Involvement of chondroitin sulfate synthase-3 (chondroitin synthase-2) in chondroitin polymerization through its interaction with

chondroitin synthase-1 or chondroitin-polymerizing factor. Biochem. J. **403**(3), 545–552 (2007). https://doi.org/10.1042/BJ20061876

11. Kitagawa, H., Izumikawa, T., Uyama, T., Sugahara, K.: Molecular cloning of a chondroitin polymerizing factor that cooperates with chondroitin synthase for chondroitin polymerization. J. Biol. Chem. **278**(26), 23666–23671 (2003). https://doi.org/10.1074/jbc.M302493200
12. Yada, T., Sato, T., Kaseyama, H., Gotoh, M., Iwasaki, H., Kikuchi, N., Kwon, Y.D., Togayachi, A., Kudo, T., Watanabe, H., Narimatsu, H., Kimata, K.: Chondroitin sulfate synthase-3: Molecular cloning and characterization. J. Biol. Chem. **278**(41), 39711–39725 (2003). https://doi.org/10.1074/jbc.M304421200
13. Mizumoto, S., Yamada, S.: An overview of in vivo functions of chondroitin sulfate and dermatan sulfate revealed by their deficient mice. Front. Cell. Dev. Biol. **9**, 764781 (2021). https://doi.org/10.3389/fcell.2021.764781
14. Cahyadi, D.D., Okamoto, M., Warita, K., Takeda-Okuda, N., Tamura, J.I., Hosaka, Y.Z.: Compositional analysis of chondroitin/dermatan sulfate in rhesus monkeys (*Macaca mulatta*). Biosci. Biotechnol. Biochem. **86**(7), 811–818 (2022). https://doi.org/10.1093/bbb/zbac057
15. Higashi, K., Takeuchi, Y., Mukuno, A., Tomitori, H., Miya, M., Linhardt, R.J., Toida, T.: Composition of glycosaminoglycans in elasmobranchs including several deep-sea sharks: Identification of chondroitin/dermatan sulfate from the dried fins of *Isurus oxyrinchus* and *Prionace glauca*. PLoS ONE. **10**(3), 1–15 (2015). https://doi.org/10.1371/journal.pone.0120860
16. Muthusamy, A., Achur, R.N., Valiyaveettil, M., Madhunapantula, S.V., Kakizaki, I., Bhavanandan, V.P., Gowda, C.D.: Structural characterization of the bovine tracheal chondroitin sulfate chains and binding of *Plasmodium falciparum*-infected erythrocytes. Glycobiology. **14**(7), 635–645 (2004). https://doi.org/10.1093/glycob/cwh077
17. Okazaki, J., Kamada, A., Gonda, Y., Sakaki, T.: Analysis of chondroitin sulfate isomers in the periodontium of the monkey using high-performance liquid chromatography. J. Periodontal Res. **27**(5), 484–488 (1992). https://doi.org/10.1111/j.1600-0765.1992.tb01821.x
18. Sundaresan, G., Abraham, R.J.J., Appa Rao, V., Narendra Babu, R., Govind, V., Meti, M.F.: Established method of chondroitin sulphate extraction from buffalo (*Bubalus bubalis*) cartilages and its identification by FTIR. J. Food Sci. Technol. **55**(9), 3439–3445 (2018). https://doi.org/10.1007/s13197-018-3253-4
19. Suzuki, Y., Kerever, A., Tanaka, T., Higashi, K., Arikawa-Hirasawa, E.: The structural and compositional changes of chondroitin sulfate chains in the aged mouse hippocampus. Juntendo Med. J. **65**(1), 64–70 (2019). https://doi.org/10.14789/jmj.2019.65.jmj18-oa13
20. Takeda-Okuda, N., Mizumoto, S., Zhang, Z., Kim, S.K., Lee, C.H., Jeon, B.T., Hosaka, Y.Z., Kadomatsu, K., Yamada, S., Tamura, J.I.: Compositional analysis of the glycosaminoglycan family in velvet antlers of sika deer (*Cervus nippon*) at different growing stages. Glycoconj. J. **36**(2), 127–139 (2019). https://doi.org/10.1007/s10719-019-09859-1

21. Takeda, N., Horai, S., Tamura, J.I.: Facile analysis of contents and compositions of the chondroitin sulfate/dermatan sulfate hybrid chain in shark and ray tissues. Carbohydr. Res. **424**, 54–58 (2016). https://doi.org/10.1016/j.carres.2016.02.006
22. Toledo, O.M.S., Dietrich, C.P.: Tissue specific distribution of sulfated mucopolysaccharides in mammals. Biochim. Biophys. Acta Gen. Subj. **498**(1), 114–122 (1977). https://doi.org/10.1016/0304-4165(77)90092-7
23. Vasan, N.S., Saporito, R.A. Jr., Saraswathi, S., Tesoriero, J.V., Manley, S.: Alterations of renal cortex and medullary glycosaminoglycans in aging dog kidney. Biochim. Biophys. Acta Gen. Subj. **760**(2), 197–205 (1983). https://doi.org/10.1016/0304-4165(83)90164-2
24. Volpi, N.: Disaccharide mapping of chondroitin sulfate of different origins by high-performance capillary electrophoresis and high-performance liquid chromatography. Carbohydr. Polym. **55**(3), 273–281 (2004). https://doi.org/10.1016/j.carbpol.2003.09.010
25. Izumikawa, T., Sato, B., Kitagawa, H.: Chondroitin sulfate is indispensable for pluripotency and differentiation of mouse embryonic stem cells. Sci. Rep. **4**, 3701 (2014). https://doi.org/10.1038/srep03701
26. Mizumoto, S., Yamada, S.: The specific role of dermatan sulfate as an instructive glycosaminoglycan in tissue development. Int. J. Mol. Sci. **23**, 7485 (2022). https://doi.org/10.3390/ijms23137485
27. Ogura, C., Hirano, K., Mizumoto, S., Yamada, S., Nishihara, S.: Dermatan sulphate promotes neuronal differentiation in mouse and human stem cells. J. Biochem. **169**(1), 55–64 (2021). https://doi.org/10.1093/jb/mvaa087
28. Sirko, S., Von Holst, A., Wizenmann, A., Götz, M., Faissner, A.: Chondroitin sulfate glycosaminoglycans control proliferation, radial glia cell differentiation and neurogenesis in neural stem/progenitor cells. Development. **134**(15), 2727–2738 (2007). https://doi.org/10.1242/dev.02871
29. Volpi, N., Bolognani, L., Conte, A., Petrini, M.: Effects of chondroitin sulfates with different structures on leukemia cells: U-937 cell proliferation and differentiation. Leuk. Res. **17**(9), 789–798 (1993). https://doi.org/10.1016/0145-2126(93)90114-Z
30. Mikami, T., Koyama, S., Yabuta, Y., Kitagawa, H.: Chondroitin sulfate is a crucial determinant for skeletal muscle development/regeneration and improvement of muscular dystrophies. J. Biol. Chem. **287**(46), 38531–38542 (2012). https://doi.org/10.1074/jbc.M111.336925
31. Rosen, E.D., MacDougald, O.A.: Adipocyte differentiation from the inside out. Nat. Rev. Mol. Cell. Biol. **7**(12), 885–896 (2006). https://doi.org/10.1038/nrm2066
32. Haupt, L.M., Murali, S., Mun, F.K., Teplyuk, N., Mei, L.F., Stein, G.S., van Wijnen, A.J., Nurcombe, V., Cool, S.M.: The heparan sulfate proteoglycan (HSPG) glypican-3 mediates commitment of MC3T3-E1 cells toward osteogenesis. J. Cell. Physiol. **220**(3), 780–791 (2009). https://doi.org/10.1002/jcp.21825
33. Mikael, P.E., Willard, C., Koyee, A., Barlao, C.G., Liu, X., Han, X., Ouyang, Y., Xia, K., Linhardt, R.J., Dordick, J.S.: Remodeling of glycosaminoglycans during differentiation of adult human bone

mesenchymal stromal cells toward hepatocytes. Stem Cells Dev. **28**(4), 278–289 (2019). https://doi.org/10.1089/scd.2018.0197

34. Nairn, A.V., Kinoshita-Toyoda, A., Toyoda, H., Xie, J., Harris, K., Dalton, S., Kulik, M., Pierce, J.M., Toida, T., Moremen, K.W., Linhardt, R.J.: Glycomics of proteoglycan biosynthesis in murine embryonic stem cell differentiation. J. Proteome Res. **6**(11), 4374–4387 (2007). https://doi.org/10.1021/pr070446f
35. Nairn, A.V., Aoki, K., dela Rosa, M., Porterfield, M., Lim, J.M., Kulik, M., Pierce, J.M., Wells, L., Dalton, S., Tiemeyer, M., Moremen, K.W.: Regulation of glycan structures in murine embryonic stem cells: Combined transcript profiling of glycan-related genes and glycan structural analysis. J. Biol. Chem. **287**(45), 37835–37856 (2012). https://doi.org/10.1074/jbc.M112.405233
36. Calvo, J.C., Rodbard, D., Katki, A., Chernick, S., Yanagishita, M.: Differentiation of 3T3-L1 preadipocytes with 3-isobutyl-1-methylxanthine and dexamethasone stimulates cell-associated and soluble chondroitin 4-sulfate proteoglycans. J. Biol. Chem. **266**(17), 11237–11244 (1991). https://doi.org/10.1016/s0021-9258(18)99154-4
37. Han, C.Y., Kang, I., Harten, I.A., Gebe, J.A., Chan, C.K., Omer, M., Alonge, K.M., Hartigh, Kjerulf, L.J.G., Goodspeed, D., Subramanian, L., Wang, S., Kim, S., Birk, F., Wight, D.E., Chait, T.N.: Adipocyte-derived versican and macrophage-derived biglycan control adipose tissue inflammation in obesity. Cell. Rep. **31**(13), 107818 (2020). https://doi.org/10.1016/j.celrep.2020.107818
38. Musil, K.J., Malmström, A., Donnér, J.: Alteration of proteoglycan metabolism during the differentiation of 3T3-L1 fibroblasts into adipocytes. J. Cell. Biol. **114**(4), 821–826 (1991). https://doi.org/10.1083/jcb.114.4.821
39. Zizola, C.F., Julianelli, V., Bertolesi, G., Yanagishita, M., Calvo, J.C.: Role of versican and hyaluronan in the differentiation of 3T3-L1 cells into preadipocytes and mature adipocytes. Matrix Biol. **26**(6), 419–430 (2007). https://doi.org/10.1016/j.matbio.2007.04.002
40. Yoshida, K., Miyauchi, S., Kikuchi, H., Tawada, A., Tokuyasu, K.: Analysis of unsaturated disaccharides from glycosaminoglycuronan by high-performance liquid chromatography. Anal. Biochem. **177**(2), 327–332 (1989). https://doi.org/10.1016/0003-2697(89)90061-4
41. Hjerpe, A., Aantonopoulos, C.A., Engfeldt, B.: Determination of hyaluronic acid using high-performance liquid chromatography of chondroitinase digests. J. Chromatogr. A. **245**(3), 365–368 (1982). https://doi.org/10.1016/S0021-9673(00)88025-5
42. Akatsu, C., Mizumoto, S., Kaneiwa, T., Maccarana, M., Malmström, A., Yamada, S., Sugahara, K.: Dermatan sulfate epimerase 2 is the predominant isozyme in the formation of the chondroitin sulfate/dermatan sulfate hybrid structure in postnatal developing mouse brain. Glycobiology. **21**(5), 565–574 (2011). https://doi.org/10.1093/glycob/cwq208
43. Cahyadi, D.D., Warita, T., Irie, N., Mizoguchi, K., Tashiro, J., Hosaka, Y.Z., Warita, K.: Housekeeping gene expression variability in differentiating and non-differentiating 3T3-L1 cells. Adipocyte. **12**(1), 2235081 (2023). https://doi.org/10.1080/21623945.2023.2235081
44. Kanda, T., Brown, J.D., Orasanu, G., Vogel, S., Gonzalez, F.J., Sartoretto, J., Michel, T., Plutzky, J.: PPARγ in the endothelium regulates metabolic responses to high-fat diet in mice. J. Clin. Investig.

119(1), 110–124 (2009). https://doi.org/10.1172/JCI36233

45. Ogawa, H., Hatano, S., Sugiura, N., Nagai, N., Sato, T., Shimizu, K., Kimata, K., Narimatsu, H., Watanabe, H.: Chondroitin sulfate synthase-2 is necessary for chain extension of chondroitin sulfate but not critical for skeletal development. PLoS ONE. **7**(8), e43806 (2012). https://doi.org/10.1371/journal.pone.0043806
46. Lyu, Z., Da, Y., Liu, H., Wang, Z., Zhu, Y., Tian, J.: Chsy1 deficiency reduces extracellular matrix productions and aggravates cartilage injury in osteoarthritis. Gene. **827**, 146466 (2022). https://doi.org/10.1016/j.gene.2022.146466
47. Myung, D., Bin, Han, H.S., Shin, J.S., Park, J.Y., Hwang, H.J., Kim, H.J., Ahn, H.S., Lee, S.H., Lee, K.T.: Hydrangenol isolated from the leaves of *Hydrangea serrata* attenuates wrinkle formation and repairs skin moisture in UVB-irradiated hairless mice. Nutrients. **11**(10), 2354 (2019). https://doi.org/10.3390/nu11102354
48. Jadin, L., Wu, X., Ding, H., Frost, G.I., Onclinx, C., Triggs-Raine, B., Flamion, B.: Skeletal and hematological anomalies in HYAL2-deficient mice: A second type of mucopolysaccharidosis IX? FASEB J. **22**(12), 4316–4326 (2008). https://doi.org/10.1096/fj.08-111997
49. Koike, T., Mikami, T., Shida, M., Habuchi, O., Kitagawa, H.: Chondroitin sulfate-E mediates estrogen-induced osteoanabolism. Sci. Rep. **5**, 8994 (2015). https://doi.org/10.1038/srep08994
50. Yoshizawa, T., Mizumoto, S., Takahashi, Y., Shimada, S., Sugahara, K., Nakayama, J., Takeda, S., Nomura, Y., Nitahara-Kasahara, Y., Okada, T., Matsumoto, K., Yamada, S., Kosho, T.: Vascular abnormalities in the placenta of *Chst14*$^{-/-}$ fetuses: Implications in the pathophysiology of perinatal lethality of the murine model and vascular lesions in human CHST14/D4ST1 deficiency. Glycobiology. **28**(2), 80–89 (2018). https://doi.org/10.1093/glycob/cwx099
51. Mizumoto, S., Watanabe, M., Yamada, S., Sugahara, K.: Expression of *N*-acetylgalactosamine 4-sulfate 6-*O*-sulfotransferase involved in chondroitin sulfate synthesis is responsible for pulmonary metastasis. BioMed Res. Int. 656319 (2013). (2013). https://doi.org/10.1155/2013/656319
52. Hosaka, Y.Z., Washie, S., Warita, K.: Preliminary study of the gene expression of sulfation and degradation enzymes for chondroitin sulfate in glycerol-treated C2C12 myoblast cells. J. Vet. Med. Sci. **84**(3), 306–309 (2022). https://doi.org/10.1292/jvms.21-0632
53. Stachtea, X.N., Tykesson, E., Van Kuppevelt, T.H., Feinstein, R., Malmström, A., Reijmers, R.M., Maccarana, M.: Dermatan sulfate-free mice display embryological defects and are neonatal lethal despite normal lymphoid and non-lymphoid organogenesis. PLoS ONE. **10**(10), –e0140279 (2015). https://doi.org/10.1371/journal.pone.0140279
54. Muñoz, J.J., Anauate, A.C., Amaral, A.G., Ferreira, F.M., Watanabe, E.H., Meca, R., Ormanji, M.S., Boim, M.A., Onuchic, L.F., Heilberg, I.P.: *Ppia* is the most stable housekeeping gene for qRT-PCR normalization in kidneys of three *Pkd1*-deficient mouse models. Sci. Rep. **11**, 19798 (2021). https://doi.org/10.1038/s41598-021-99366-x
55. Maccarana, M., Kalamajski, S., Kongsgaard, M., Magnusson, S.P., Oldberg, Ã., Malmström, A.: Dermatan sulfate epimerase 1-deficient mice have reduced content and changed distribution of

iduronic acids in dermatan sulfate and an altered collagen structure in skin. Mol. Cell. Biol. **29**(20), 5517–5528 (2009). https://doi.org/10.1128/mcb.00430-09

56. Pacheco, B., Malmström, A., Maccarana, M.: Two dermatan sulfate epimerases form iduronic acid domains in dermatan sulfate. J. Biol. Chem. **284**(15), 9788–9795 (2009). https://doi.org/10.1074/jbc.M809339200
57. Kolset, S.O., Ivhed, I., Øvervatn, A., Nilsson, K.: Differentiation-associated changes in the expression of chondroitin sulfate proteoglycan in induced U-937 cells. Cancer Res. **48**(21), 6103–6108 (1988)
58. Laskin, J.D., Dokidis, A., Sirak, A.A., Laskin, D.L.: Distinct patterns of sulfated proteoglycan biosynthesis in human monocytes, granulocytes and myeloid leukemic cells. Leuk. Res. **15**(6), 515–523 (1991). https://doi.org/10.1016/0145-2126(91)90063-Y
59. Reiss, M., Maniglia, C.A., Sartorelli, A.C.: Reversible effects of retinoic acid on glycosaminoglycan synthesis during differentiation of HL-60 leukemia cells. Cancer Res. **45**(5), 2092–2097 (1985)
60. Leal, A.F., Benincore-Flórez, E., Rintz, E., Herreño-Pachón, A.M., Celik, B., Ago, Y., Alméciga-Díaz, C.J., Tomatsu, S.: Mucopolysaccharidoses: Cellular consequences of glycosaminoglycans accumulation and potential targets. Int. J. Mol. Sci. **24**(1), 477 (2023). https://doi.org/10.3390/ijms24010477
61. Ambele, M.A., Dessels, C., Durandt, C., Pepper, M.S.: Genome-wide analysis of gene expression during adipogenesis in human adipose-derived stromal cells reveals novel patterns of gene expression during adipocyte differentiation. Stem Cell. Res. **16**(3), 725–734 (2016). https://doi.org/10.1016/j.scr.2016.04.011
62. Izumikawa, T., Koike, T., Shiozawa, S., Sugahara, K., Tamura, J.I., Kitagawa, H.: Identification of chondroitin sulfate glucuronyltransferase as chondroitin synthase-3 involved in chondroitin polymerization: Chondroitin polymerization is achieved by multiple enzyme complexes consisting of chondroitin synthase family members. J. Biol. Chem. **283**(17), 11396–11406 (2008). https://doi.org/10.1074/jbc.M707549200
63. Mikami, T., Kitagawa, H.: Biosynthesis and function of chondroitin sulfate. Biochim. Biophys. Acta Gen. Subj. **1830**(10), 4719–4733 (2013). https://doi.org/10.1016/j.bbagen.2013.06.006
64. Gushulak, L., Hemming, R., Martin, D., Seyrantepe, V., Pshezhetsky, A., Triggs-Raine, B.: Hyaluronidase 1 and β-hexosaminidase have redundant functions in hyaluronan and chondroitin sulfate degradation. J. Biol. Chem. **287**(20), 16689–16697 (2012). https://doi.org/10.1074/jbc.M112.350447
65. Honda, T., Kaneiwa, T., Mizumoto, S., Sugahara, K., Yamada, S.: Hyaluronidases have strong hydrolytic activity toward chondroitin 4-sulfate comparable to that for hyaluronan. Biomolecules. **2**(4), 549–563 (2012). https://doi.org/10.3390/biom2040549
66. Yamada, S., Mizumoto, S.: Characterization of hyaluronidase 4 involved in the catabolism of chondroitin sulfate. Molecules. **27**(18), 6103 (2022). https://doi.org/10.3390/molecules27186103
67. Higashi, K.: Expression of glycosaminoglycan-related genes and the role of polyamines in the glycosaminoglycan biosynthetic pathways. Trends Glycosci. Glycotechnol. **32**(189), E167–E175 (2020). https://doi.org/10.4052/tigg.1979.7E

68. Hiraoka, N., Nakagawa, H., Ong, E., Akama, T.O., Fukuda, M.N., Fukuda, M.: Molecular cloning and expression of two distinct human chondroitin 4-*O*-sulfotransferases that belong to the HNK-1 sulfotransferase gene family. J. Biol. Chem. **275**(26), 20188–20196 (2000). https://doi.org/10.1074/jbc.M002443200
69. Miyake, N., Kosho, T., Mizumoto, S., Furuichi, T., Hatamochi, A., Nagashima, Y., Arai, E., Takahashi, K., Kawamura, R., Wakui, K., Takahashi, J., Kato, H., Yasui, H., Ishida, T., Ohashi, H., Nishimura, G., Shiina, M., Saitsu, H., Tsurusaki, Y., Doi, H., Fukushima, Y., Ikegawa, S., Yamada, S., Sugahara, K., Matsumoto, N.: Loss-of-function mutations of CHST14 in a new type of Ehlers-Danlos syndrome. Hum. Mutat. **31**(8), 966–974 (2010). https://doi.org/10.1002/humu.21300
70. Pacheco, B., Maccarana, M., Malmström, A.: Dermatan 4-*O*-sulfotransferase 1 is pivotal in the formation of iduronic acid blocks in dermatan sulfate. Glycobiology. **19**(11), 1197–1203 (2009). https://doi.org/10.1093/glycob/cwp110
71. Ito, Y., Habuchi, O.: Purification and characterization of *N*-acetylgalactosamine 4-sulfate 6-*O*-sulfotransferase from the squid cartilage. J. Biol. Chem. **275**(44), 34728–34736 (2000). https://doi.org/10.1074/jbc.M909633199
72. Ohtake, S., Kimata, K., Habuchi, O.: A unique nonreducing terminal modification of chondroitin sulfate by *N*-acetylgalactosamine 4-sulfate 6-*O*-sulfotransferase. J. Biol. Chem. **278**(40), 38443–38452 (2003). https://doi.org/10.1074/jbc.M306132200
73. Kobayashi, M., Sugumaran, G., Liu, J., Shworak, N.W., Silbert, J.E., Rosenberg, R.D.: Molecular cloning and characterization of a human uronyl 2-sulfotransferase that sulfates iduronyl and glucuronyl residues in dermatan/chondroitin sulfate. J. Biol. Chem. **274**(15), 10474–10480 (1999). https://doi.org/10.1074/jbc.274.15.10474

Figures

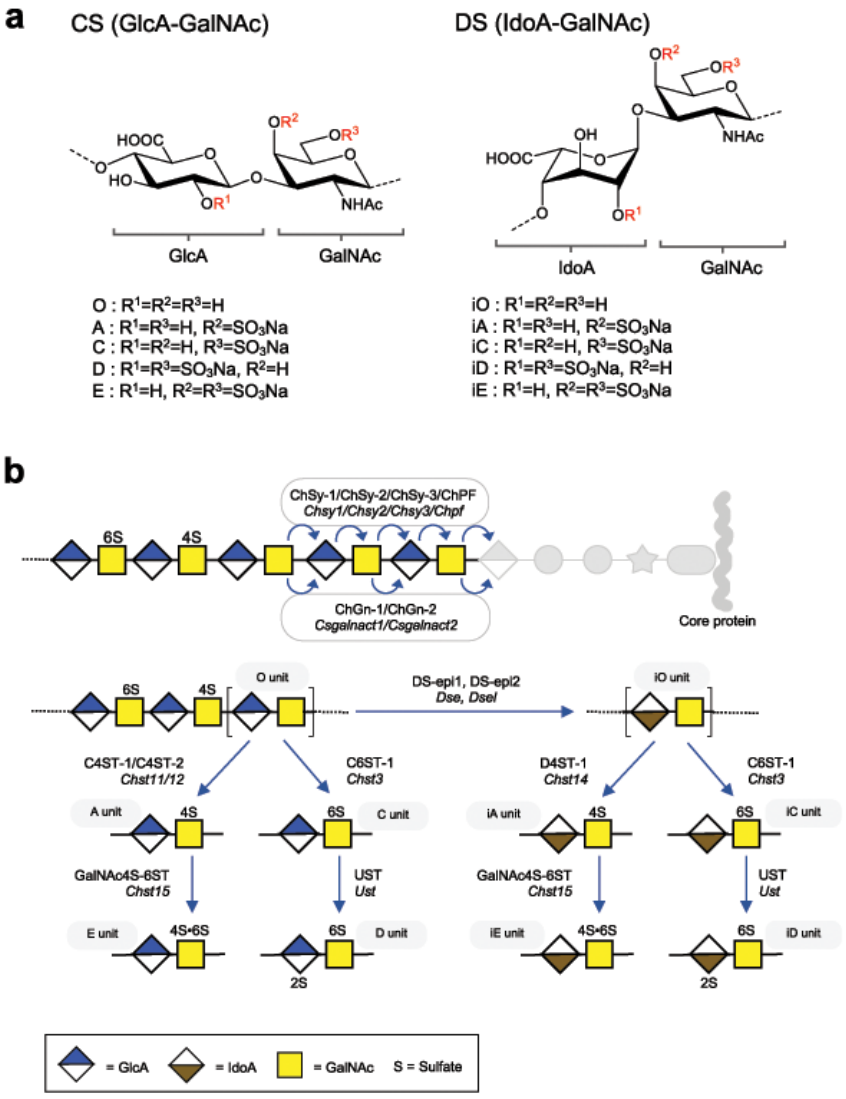

Figure 1

Structure and biosynthesis of CS and DS. (**a**) The chemical structure of CS and DS disaccharides repeating units comprise GlcA or IdoA, and GalNac. (**b**) Schematic diagram of CS/DS biosynthesis. A number of glycosyltransferases catalyze chain initiation and elongation, as well as participate in chondroitin polymerization. Several sulfotransferases catalyze the sulfation at various positions in CS/DS, resulting in the formation of different CS/DS types. Abbreviation: GlcA, glucuronic acid; GalNAc,

N-acetylgalactosamine; IdoA , iduronic acid; ChSy, chondroitin synthase; ChPF, chondroitin polymerizing factor; ChGn, chondroitin GalNac transferase; C4ST, chondroitin 4-*O*-sulfotransferase; C6ST, chondroitin 6-*O*-sulfotransferase; GalNAc4S-6ST, GalNAc 4-sulfate 6-*O*-sulfotransferase; UST, uronyl 2-*O*-sulfotransferase; D4ST, dermatan 4-*O*-sulfotransferase; DS-epi, glucuronyl C-5 epimerase; *Chsy*, chondroitin sulfate synthase; *Chpf*, chondroitin polymerizing factor; *Csgalnact*, chondroitin sulfate *N*-acetylgalactosaminyltransferase; *Chst*, carbohydrate sulfotransferase; *Ust*, uronyl-2-sulfotransferase

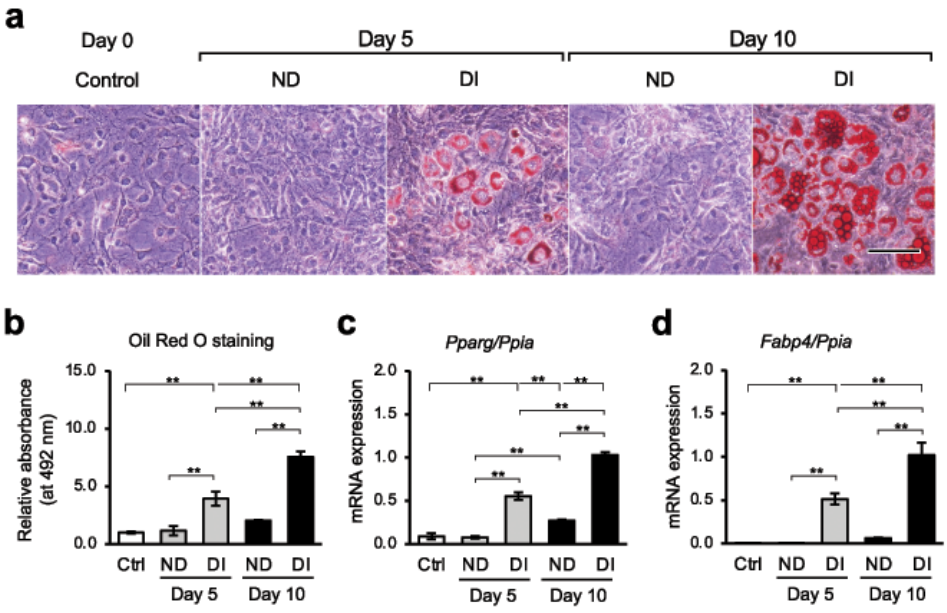

Figure 2

Semi-quantitative Oil Red O (ORO) staining and adipogenesis transcription factors-related gene expression analysis confirms the adipocyte differentiation. (**a**) Lipid droplet accumulation was observed in the differentiated (DI) groups, on days 5 and 10 post-differentiation induction. Scale bar = 100 µm. (**b**) Accumulation of lipid droplets was observed in the differentiated 3T3-L1 cells of the DI groups. The absorbance of the eluted ORO obtained from the stained oil droplets was measured using a microplate reader at 492 nm. **P < 0.01 using Bonferroni test. (**c**) *Pparg* and (**d**) *Fabp4* expression per 50 ng of total RNA in all experimental groups. The mRNA expression of both *Pparg* and *Fabp4* in the DI groups was higher than in the ND groups. **P < 0.01 using Bonferroni test. Data are presented as the mean ± standard deviation (SD) of triplicate samples

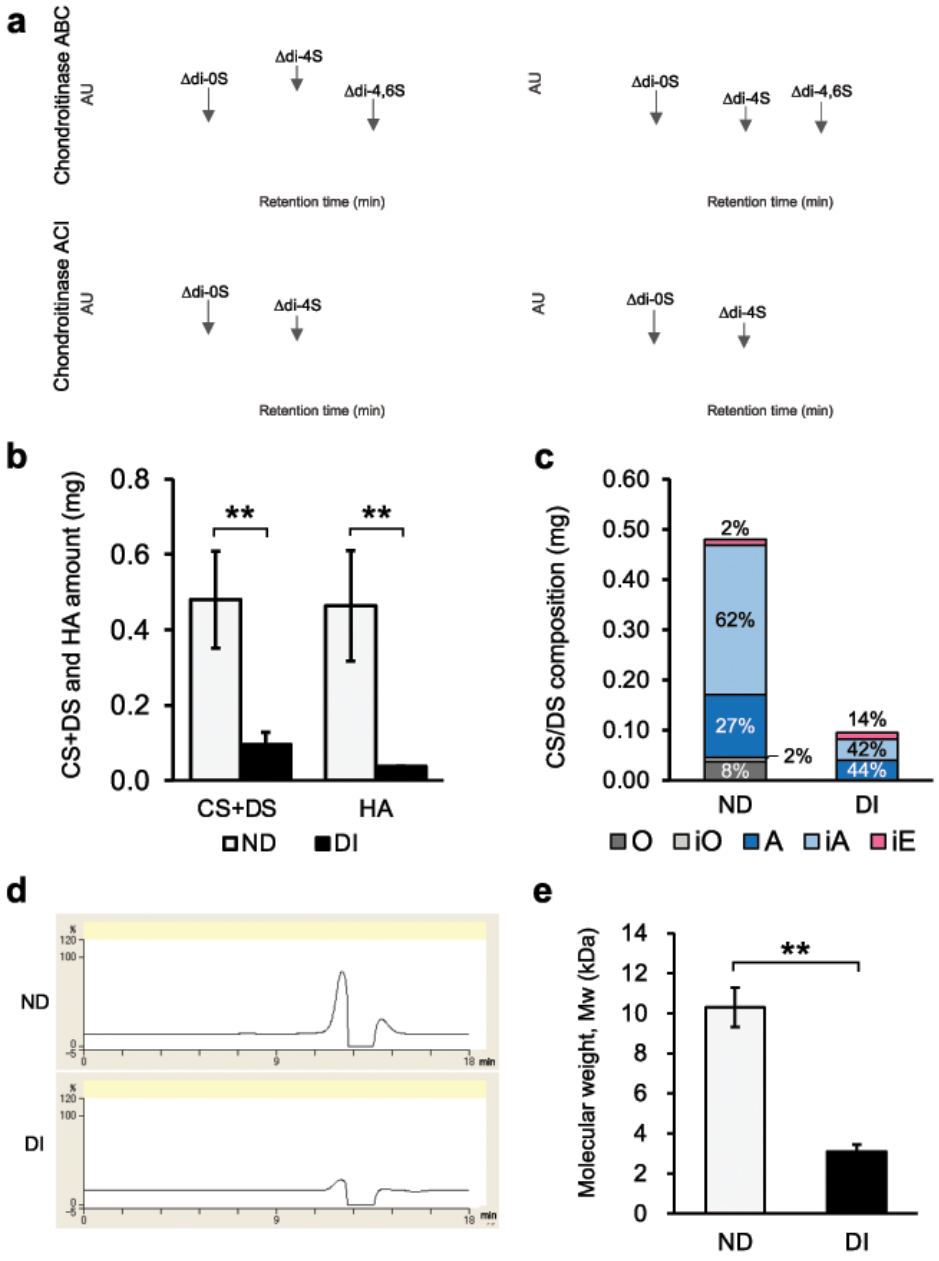

Figure 3

Glycosaminoglycans (GAGs) contents, composition of CS/DS types, and its molecular weight. (**a**) Representative chromatograms of the unsaturated disaccharides obtained from the chondroitinase digestion detected in the 3T3-L1 cells of the non-differentiated (ND) and differentiated (DI) groups. The elution positions of unsaturated disaccharides are indicated: Δdi-0S, ΔHexAα1-3GalNAc (ΔO unit); Δdi-4S, ΔHexAα1-3GalNAc(4S) (ΔA unit); Δdi-4,6S, ΔHexAα1-3GalNAc(4S,6S) (ΔE unit). (**b**) CS+DS and HA

contents were reduced in the DI group compared to the ND group. **P < 0.01 using an unpaired two-tailed *t*-test. (**c**) Composition of the CS/DS types in the ND and DI groups. ΔA unitwas the major CS/DS disaccharide found in 3T3-L1 cells, although the alteration of the CS/DS types composition was observed in the DI group compared to the ND group. (**d**) Representative chromatograms of the non-differentiating and differentiating 3T3-L1 cells-derived GAGs molecular weight measurement. (**e**) The molecular weight of the GAGs in the ND and DI groups. The results indicate a reduction in the chain length of GAGs in the DI group. **P < 0.01 using an unpaired two-tailed *t*-test. Data are presented as the mean ± standard deviation (SD) of triplicate samples.

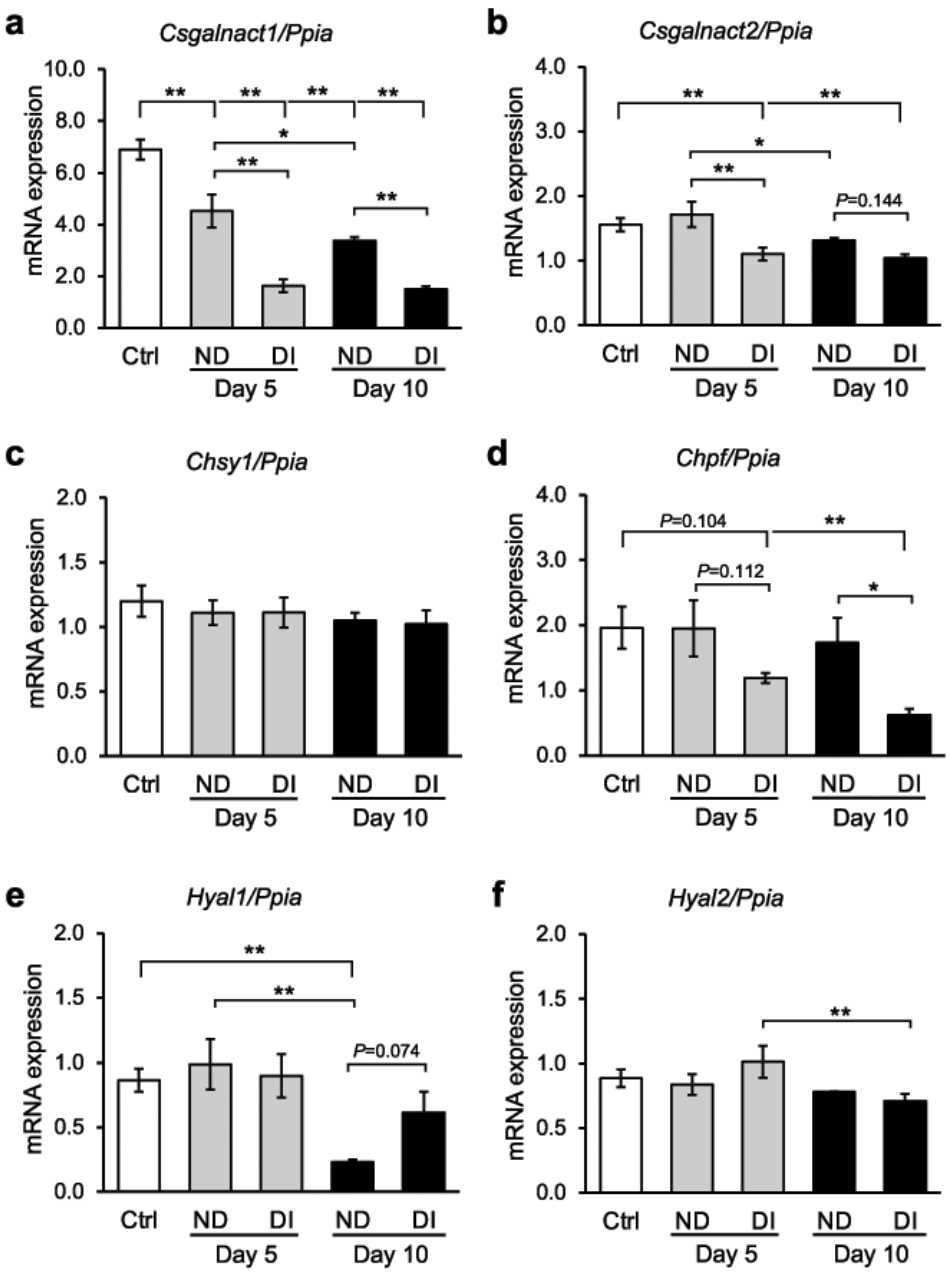

Figure 4

Decreased mRNA expression encoding ChGn-1 and -2 (*Csgalnact1*and *Csgalnact2*) and ChPF (*Chpf*) in the DI group compared to the ND and control group. The mRNA expression of glycosyltransferases-encoding genes (**a**) *Csgalnact1*, (**b**) *Csgalnact2*, (**c**) *Chsy1*, (**d**) *Chpf*, and CS hydrolases-encoding genes (**e**) *Hyal1*and (f) *Hyal2*. *P < 0.05 and **P < 0.01 using Bonferroni test. Data are presented as the mean ± standard deviation (SD) of triplicate samples.

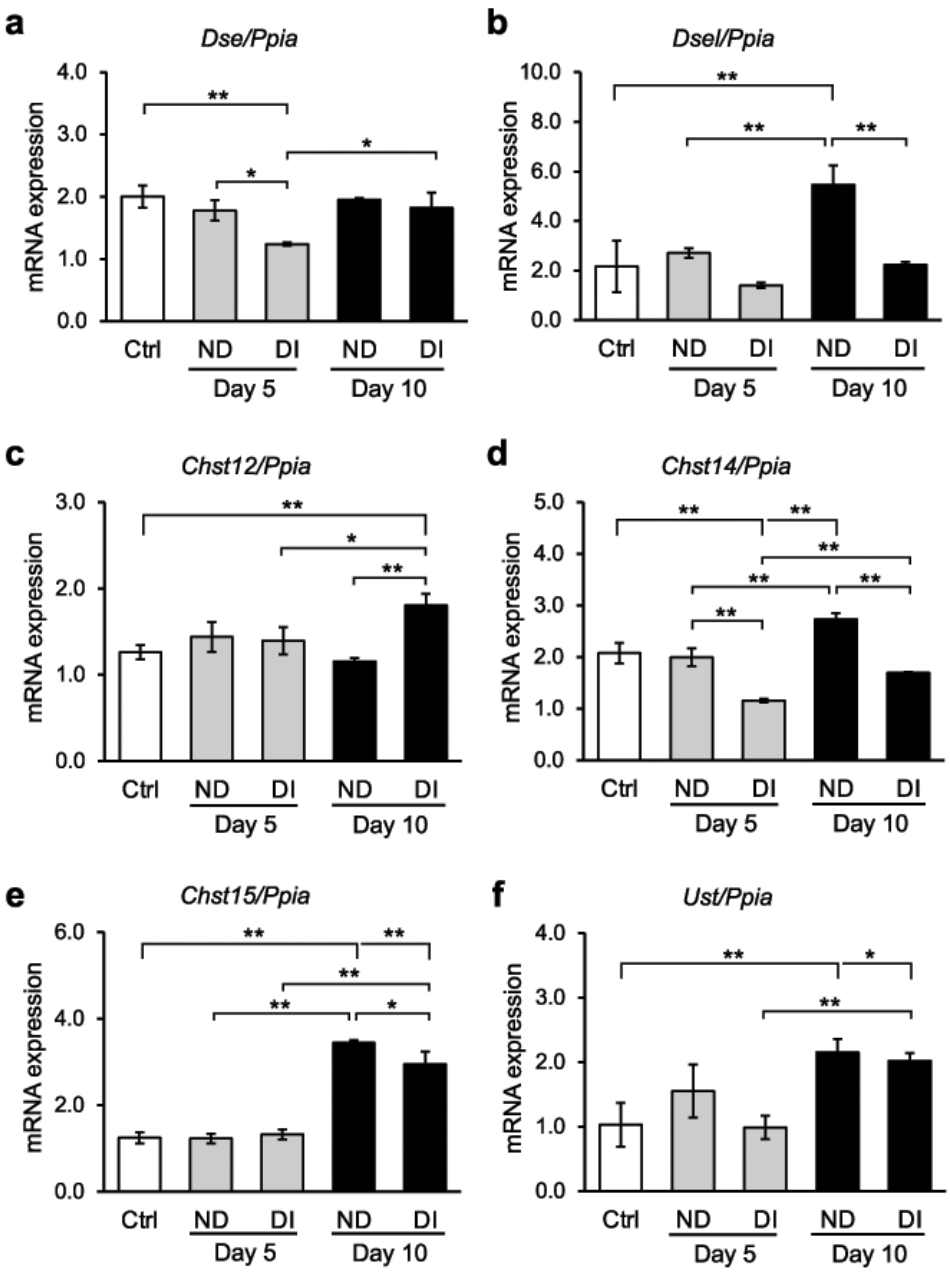

Figure 5

mRNA expression levels of genes encoding DS epimerases and sulfotransferases in the non-differentiating and differentiating 3T3-L1 cells. The mRNA expression of (**a**) *Dse*, (**b**) *Dsel*, (**c**) *Chst12*, (**d**) *Chst14*, (**e**) *Chst15*, (**f**) *Ust*. *P < 0.05 and **P < 0.01 using Bonferroni test. Data are presented as the mean ± standard deviation (SD) of triplicate samples.

Supplementary Files

This is a list of supplementary files associated with this preprint. Click to download.

- CahyadiSupplTable1.docx